

**AFRL-PR-WP-TP-2005-201**

**PREDICTING TRANSITION IN  
TURBOMACHINERY**

**Part I - A Review and New Model  
Development**



**J.P. Clark  
T.J. Praisner**

**APRIL 2005**

**Approved for public release; distribution is unlimited.**

**STINFO FINAL REPORT**

**This work has been submitted to the American Society of Mechanical Engineers (ASME) for publication in the Proceedings of the Turbo Expo 2004. One of the authors is a U.S. Government employee; therefore, the U.S. Government is joint owner of the work. If published, ASME may assert copyright. If so, the United States has for itself and others acting on its behalf an unlimited, paid-up, nonexclusive, irrevocable worldwide license to use, modify, reproduce, release, perform, display or disclose the work by or on behalf of the Government. Any other form of use is subject to copyright restrictions.**

**PROPULSION DIRECTORATE  
AIR FORCE MATERIEL COMMAND  
AIR FORCE RESEARCH LABORATORY  
WRIGHT-PATTERSON AIR FORCE BASE, OH 45433-7251**

## NOTICE

Using Government drawings, specifications, or other data included in this document for any purpose other than Government procurement does not in any way obligate the U.S. Government. The fact that the Government formulated or supplied the drawings, specifications, or other data does not license the holder or any other person or corporation; or convey any rights or permission to manufacture, use, or sell any patented invention that may relate to them.

This report was cleared for public release by the Air Force Research Laboratory Wright Site Public Affairs Office (AFRL/WS) and is releasable to the National Technical Information Service (NTIS). It will be available to the general public, including foreign nationals.

THIS TECHNICAL REPORT IS APPROVED FOR PUBLICATION.

/s/

---

RYAN P. LEMAIRE, Lt, USAF  
Turbine Design Engineer  
Turbine Engine Division

/s/

---

CHARLES W. STEVENS  
Chief, Turbine Branch  
Turbine Engine Division

/s/

---

~~JEFFREY~~ M. STRICKER  
Chief Engineer  
Turbine Engine Division  
Propulsion Directorate

This report is published in the interest of scientific and technical information exchange and its publication does not constitute the Government's approval or disapproval of its ideas or findings.

<b>REPORT DOCUMENTATION PAGE</b>				<i>Form Approved</i> OMB No. 0704-0188	
The public reporting burden for this collection of information is estimated to average 1 hour per response, including the time for reviewing instructions, searching existing data sources, gathering and maintaining the data needed, and completing and reviewing the collection of information. Send comments regarding this burden estimate or any other aspect of this collection of information, including suggestions for reducing this burden, to Department of Defense, Washington Headquarters Services, Directorate for Information Operations and Reports (0704-0188), 1215 Jefferson Davis Highway, Suite 1204, Arlington, VA 22202-4302. Respondents should be aware that notwithstanding any other provision of law, no person shall be subject to any penalty for failing to comply with a collection of information if it does not display a currently valid OMB control number. <b>PLEASE DO NOT RETURN YOUR FORM TO THE ABOVE ADDRESS.</b>					
<b>1. REPORT DATE (DD-MM-YY)</b> April 2005		<b>2. REPORT TYPE</b> Conference Paper Preprint		<b>3. DATES COVERED (From - To)</b> 06/14/2004 – 06/17/2004	
<b>4. TITLE AND SUBTITLE</b> PREDICTING TRANSITION IN TURBOMACHINERY Part I - A Review and New Model Development				<b>5a. CONTRACT NUMBER</b> In-house	
				<b>5b. GRANT NUMBER</b>	
				<b>5c. PROGRAM ELEMENT NUMBER</b> 62203F	
<b>6. AUTHOR(S)</b> J.P. Clark (AFRL/PRTT) T.J. Praisner (United Technologies Pratt & Whitney)				<b>5d. PROJECT NUMBER</b> 3066	
				<b>5e. TASK NUMBER</b> 06	
				<b>5f. WORK UNIT NUMBER</b> W8	
<b>7. PERFORMING ORGANIZATION NAME(S) AND ADDRESS(ES)</b> Turbine Branch (AFRL/PRTT) Turbine Engine Division Propulsion Directorate Air Force Research Laboratory, Air Force Materiel Command Wright-Patterson Air Force Base, OH 45433-7251				United Technologies Pratt & Whitney Turbine Aerodynamics and Durability 400 Main St., M/S 169-29 East Hartford, CT 06108	
<b>9. SPONSORING/MONITORING AGENCY NAME(S) AND ADDRESS(ES)</b> Propulsion Directorate Air Force Research Laboratory Air Force Materiel Command Wright-Patterson AFB, OH 45433-7251				<b>10. SPONSORING/MONITORING AGENCY ACRONYM(S)</b> AFRL/PRTT	
				<b>11. SPONSORING/MONITORING AGENCY REPORT NUMBER(S)</b> AFRL-PR-WP-TP-2005-201	
<b>12. DISTRIBUTION/AVAILABILITY STATEMENT</b> Approved for public release; distribution is unlimited.					
<b>13. SUPPLEMENTARY NOTES</b> This work has been submitted to the American Society of Mechanical Engineers (ASME) for publication in the Proceedings of the Turbo Expo 2004. One of the authors is a U.S. Government employee; therefore, the U.S. Government is joint owner of the work. If published, ASME may assert copyright. If so, the United States has for itself and others acting on its behalf an unlimited, paid-up, nonexclusive, irrevocable worldwide license to use, modify, reproduce, release, perform, display or disclose the work by or on behalf of the Government. Any other form of use is subject to copyright restrictions.  Report contains color. Proceedings of the IGTI: ASME Turbo Expo 14-17 June 2004, Vienna, Austria.					
<b>14. ABSTRACT</b> Here we report on an effort to include an empirically based transition modeling capability in a RANS solver. Testing of well known empirical models from literature for both attached- and separated-flow transition against cascade data revealed that the models did not provide enough fidelity for implementation in an airfoil design system. A CFD-supplemented database of experimental cascade cases (57 with attached-flow transition and 47 with separation and turbulent reattachment) was constructed to explore the development of new correlations. Dimensional analyses were performed to guide the work and appropriate non-dimensional parameters were then extracted from CFD predictions of the laminar boundary layers existing on the airfoil surfaces prior to either transition onset or incipient separation. For attached-flow transition, exploration of the database revealed a distinct correlation between local levels of freestream turbulence intensity, turbulence length scale, and momentum-thickness Reynolds number at transition onset. It was found that the correlation could be recast as a ratio of the boundary-layer diffusion time to a time-scale associated with the energy-bearing turbulent eddies. In the case of separated flow transition, it was found that the length of a separation bubble prior to turbulent re-attachment was a simple function of the local momentum thickness at separation and the overall surface length traversed by a fluid element prior to separation.					
<b>15. SUBJECT TERMS</b>					
<b>16. SECURITY CLASSIFICATION OF:</b>			<b>17. LIMITATION OF ABSTRACT:</b> SAR	<b>18. NUMBER OF PAGES</b> 20	<b>19a. NAME OF RESPONSIBLE PERSON (Monitor)</b> Ryan P. Lemaire <b>19b. TELEPHONE NUMBER (Include Area Code)</b> (937) 255-7150
<b>a. REPORT</b> Unclassified	<b>b. ABSTRACT</b> Unclassified	<b>c. THIS PAGE</b> Unclassified			



GT-2004-54108

## Predicting Transition in Turbomachinery, Part I – A Review and New Model Development

T. J. Praisner

Turbine Aerodynamics and Durability  
United Technologies Pratt & Whitney  
400 Main St., M/S 169-29  
East Hartford, CT 06108

J. P. Clark

Turbine Branch, Turbine Engine Division  
Propulsion Directorate  
Air Force Research Laboratory  
Building 18, Room 136D  
1950 5<sup>th</sup> St., WPAFB, OH 45433

### ABSTRACT

Here we report on an effort to include an empirically based transition modeling capability in a RANS solver. Testing of well-known empirical models from literature for both attached- and separated-flow transition against cascade data revealed that the models did not provide enough fidelity for implementation in an airfoil design system. Consequently, a program was launched to develop models that would provide sufficient accuracy for use in an airfoil design system. As a first step in the effort, accurate modeling of freestream turbulence development was identified as a need for any form of transition modeling capability. Additionally, capturing the effects of freestream turbulence on pre-transitional boundary layers was found to have a significant effect on the accuracy of transition modeling. A CFD-supplemented database of experimental cascade cases (57 with attached-flow transition and 47 with separation and turbulent reattachment) was constructed to explore the development of new correlations. Dimensional analyses were performed to guide the work and appropriate non-dimensional parameters were then extracted from CFD predictions of the laminar boundary layers existing on the airfoil surfaces prior to either transition onset or incipient separation. For attached-flow transition, exploration of the database revealed a distinct correlation between local levels of freestream turbulence intensity, turbulence length scale, and momentum-thickness Reynolds number at transition onset. It was found that the correlation could be recast as a ratio of the boundary-layer diffusion time to a time-scale associated with the energy-bearing turbulent eddies. In the case of separated-flow transition, it was found that the length of a separation bubble prior to turbulent re-attachment was a simple function of the local momentum thickness at separation and the overall surface length traversed by a fluid element prior to separation. Both the attached- and separated-flow transition models were implemented into the design system as point-like trips.

### INTRODUCTION

In axial-flow turbomachinery, the design trend is toward increasing airfoil loading in an effort to reduce weight and cost of future systems. Transition prediction is critical for accurate loss predictions of high lift airfoils, and the full multi-moded (Mayle, 1991) nature of the transition process must be considered. Lakshminarayana (1991), Simoneau and Simon (1993), Simon and Ashpis (1996), Dunn (2001), and Yaras (2002) all provide detailed reviews of the state of

the art in predictive techniques for turbomachinery, and they point to the need for improved models for transition.

Elevated levels of freestream turbulence ( $Tu > 1.0\%$ ) have a significant effect on pre-transitional, or quasi-laminar boundary layers. Further to that, it is the authors' opinion that the quality of the laminar boundary layer at transition onset must be captured accurately before any form of transition modeling can be employed. Therefore, it is important to capture accurately the field-wise development of freestream turbulence quantities. To that end, the ability of the  $k-\omega$  turbulence model of Wilcox (1998) to predict the development of  $Tu$  was validated against the experimental data of Ames (1994). Additionally, an accurate technique for modeling the effects of  $Tu$  on laminar boundary layers within the framework of the  $k-\omega$  model was developed.

In testing against cascade data it was found that open-literature models for attached and separated-flow transition were not sufficiently accurate for implementation in a design system. Consequently, an effort was launched to develop new correlations for attached- and separated-flow transition. A dimensional analysis was performed considering all transition-relevant quantities available within the frame-work of a RANS simulation performed with a two-equation turbulence model. A database of the resulting dimensionless groups was constructed from open-literature and Pratt & Whitney in-house cascade data. The cascade data were supplemented with quantities based on the aforementioned modeling techniques for freestream turbulence development and its effects on laminar boundary layers. An investigation of the resulting database enabled the development of new models for attached- and separated-flow transition. The details of this process are documented below.

A computational-methods section will be presented first with discussions on boundary conditions, freestream-disturbance propagation and quasi-laminar boundary layers. Then, sections concerning attached- and separated-flow transition are presented, where reviews of the state-of-the-art and current model development details are discussed. Validation and benchmarking of the new models is presented in Part II of this manuscript.

### COMPUTATIONAL METHODS

Steady-state and time-resolved turbine flowfields were predicted using the 3-D, Reynolds-Averaged Navier-Stokes (RANS) code described both by Ni (1999) and Davis et al. (1996). Numerical



closure for turbulent flow is obtained via the  $k$ - $\omega$  turbulence model due to Wilcox (1998). An O-H grid topology was employed for all simulations, and approximately 600,000 grid points per passage were used for three-dimensional simulations executed for this study (without tip clearance). The viscous-grid provides near-surface values of  $y^+$  less than 1 over all no-slip boundaries and gives approximately 7 grid points per momentum thickness in airfoil and endwall boundary layers. These grid densities and spacings are consistent with Pratt & Whitney standard work criteria defined by Praisner and Rangwalla (2001) to capture thermal fields, surface heat transfer and transition-related streamwise gradients in gas turbines. The code is accurate to second-order in space and time and multi-grid techniques are used to obtain rapid convergence. Constant temperature, constant heat flux and adiabatic-wall thermal boundary conditions are available and were employed when appropriate. The inlet boundary conditions used for each simulation are described below.

### The Development of Freestream Disturbances

Freestream disturbances have been shown to play an important role in transition (See e.g. Abu Ghannam and Shaw 1980, and Mayle, 1991). In order to develop a RANS-based transition-modeling system, some form of freestream turbulence modeling must be implemented in the solver. Two-equation turbulence models, which provide modeling of the convection, dissipation, and diffusion of freestream disturbances, are currently the state of the art in turbomachinery design systems. However, the ability of any two-equation model to capture accurately the development of freestream turbulence quantities in prototypical turbomachinery flowfields should be demonstrated before empirical modeling based on freestream disturbances can be applied.

Two-equation turbulence models present the user with two quantities that must be specified at the inlet of a simulation. 1) The turbulence kinetic energy,  $k$ , is directly proportional to the local turbulence intensity and velocity and, when simulating experimental data, is typically set based on measured levels. 2) The dissipation parameter should be set to match the experimental decay rate of freestream turbulence when it is derivable from published data. When it is necessary to estimate inlet boundary conditions for two-equation turbulence models, there are a number of techniques that may be employed.

When simplifications for zero pressure-gradient steady flow are applied to the  $k$ - $\omega$  equations (Wilcox, 1988) one can obtain the following relations for the freestream development of  $k$  and  $\omega$ :

$$k(x) = k_{in} \left( \frac{1}{\omega_{in}} \right)^{1.2} \left[ \frac{3x/40}{U_{\infty}} + \frac{1}{\omega_{in}} \right]^{-1.2} \quad (1)$$

$$\omega(x) = \left( \frac{3x/40}{U_{\infty}} + \frac{1}{\omega_{in}} \right)^{-1} \quad (2)$$

where  $x$  is streamwise distance,  $k_{in}$  and  $\omega_{in}$  are inlet quantities, and  $U_{\infty}$  is the freestream velocity. If the measured turbulence decay rate upstream of the cascade is known, equations 1 and 2 can be used to solve for the inlet values of  $k$  and  $\omega$ . The predicted decay rate of freestream turbulence obtained from equations 1 and 2 varies with  $x$  to the  $-0.62$  power, and this falls within the range of  $-0.60$  to  $-0.68$  reported by Baines and Peterson (1951) and Hinze (1975).

If the freestream turbulence decay rate upstream of the test section is not known then there are three other means of deriving the inlet value of the specific dissipation rate,  $\omega_{in}$ . Firstly, if the decay rate

is not reported for a configuration with grid generated turbulence, and either the grid location, or the bar size of the grid is known, then the decay rate can be estimated quite accurately by using the following relation which is similar to one from Baines and Peterson (1951):

$$Tu(x) = 1.12 \left( \frac{x}{d} \right)^{-0.65} \quad (3)$$

Here  $d$  is the cross-stream dimension of the bar elements that comprise the grid. If the experimentally estimated dissipation rate is available, the inlet value for  $\omega$  can be estimated based on the relation from Wilcox (1998):

$$\omega = \frac{2}{3} \frac{\varepsilon}{C_{\mu} u'^2} \quad (4)$$

where  $\varepsilon$  is the measured dissipation rate and  $C_{\mu}=0.09$ .

Finally, as a third, less-preferred methodology, the authors have found that the following relation from Wilcox (1998) gives a reasonable estimate for  $\omega$  at the inlet in cases where the length scale for an experimental configuration is reported as well as the inlet turbulence level:

$$\omega = \frac{u'}{C_{\mu} \lambda} \quad (5)$$

where  $\lambda$  is the measured length scale and  $u'$  is deduced from the freestream turbulence level. Use of equation 5 for grid-generated turbulence typically results in inlet values for  $\omega$  close to those obtained with equation 1.

Using these techniques for deriving  $k$  and  $\omega$  boundary conditions, comparisons were made between CFD simulations with the  $k$ - $\omega$  model and the measured freestream development of turbulence quantities in the vane cascade from Ames (1994) and Ames and Plesniak (1995). In his reports, Ames provides detailed measurements of turbulence quantities within the passage of the C3X vane. In one case freestream turbulence was generated with a passive grid, providing a turbulence intensity of 8% nominally at the inlet to the cascade. This test case is a good compromise between configuration accuracy and completeness of measured flow quantities for this type of benchmarking.

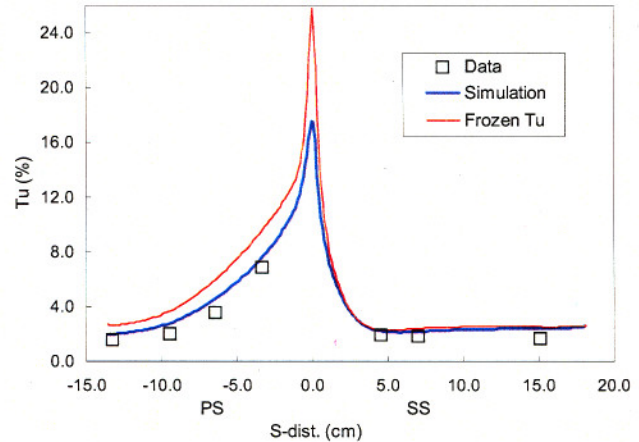


Figure 1. Measured and predicted distributions of freestream turbulence around the C3X airfoil. Data is from Ames (1994).

Figure 1 is a comparison of the measured and predicted turbulence levels around the airfoil. Also shown is the distribution of  $Tu$  obtained if "frozen" turbulence is assumed within the passage.



Frozen turbulence assumes that only the airfoil velocity distribution affects the local  $Tu$  level. This method results in over-predictions of local levels of  $Tu$  of up to 40% on the pressure side and in the stagnation region while giving good estimates on the suction side. Overall, better agreement is obtained with the freestream modeling supplied by the  $k-\omega$  model. Although, experimentally, the isotropy of the freestream turbulence is significantly reduced by the potential field of the airfoil, the evolution of the simulated *isotropic* turbulence is within  $\pm 0.5\%$  of the measured levels based on the stream-wise component of turbulence on both the pressure and suction sides of the airfoil.

For accurate multi-row modeling of multi-stage turbomachinery turbulence fields, it is also important to capture accurately the development of the turbulence length scale/dissipation rate. Figure 2 is a comparison of the predicted and experimentally estimated dissipation rates around the airfoil tested by Ames (1994). While the agreement between CFD and data is not as good here as in Figure 1, it is shown in Part II of the present work that this level of fidelity is indeed adequate for making multi-row predictions of attached- and separated-flow transition. Further, predicting the development of freestream turbulence through a turbine passage as in Figure 1 is itself dependant upon accurately calculating the rate of turbulence dissipation as the flow proceeds downstream. Again, further validation of the ability of the  $k-\omega$  model to predict the development of freestream disturbances in multi-stage environments will be presented in Part II of this paper.

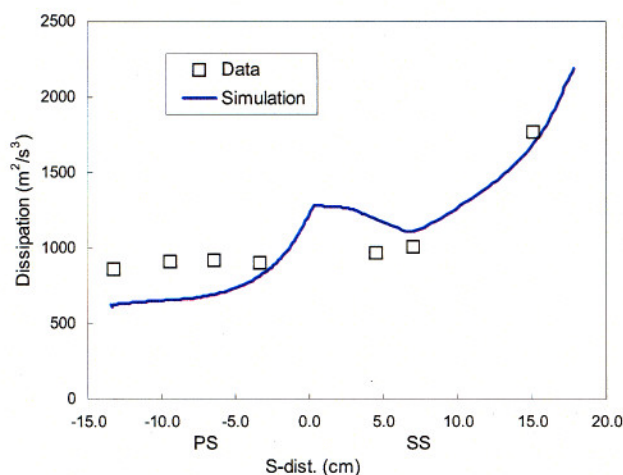


Figure 2. Comparison of measured and predicted turbulence dissipation around the C3X airfoil. Data is from Ames (1994).

### Modeling Pre-Transitional Boundary Layers

Moss and Oldfield (1992) concluded from their experimental study of turbulence level and length scale on heat transfer in laminar boundary layers that, "accurate prediction of heat transfer enhancement due to freestream turbulence is not possible using the turbulence level alone." Considering Reynolds' analogy, it seems that accurate predictions of quasi-laminar thermal and momentum boundary layers can not be obtained without attention to turbulence length scale (i.e. specific dissipation) as well as intensity.

The importance of capturing turbulence intensity and length-scale effects on laminar boundary layers was emphasized in the recent report of Boyle et al. (2003) who developed a model that considers both

turbulence level and length scale to increase turbulent viscosity above zero in laminar regions to account for what they refer to as "turbulence enhancement." Boyle and coworkers found a "noticeable" improvement in spatially averaged laminar-region heat transfer predictions using their model, but no model tested produced accurate local heat load levels. Similarly, Roach and Brierley (2000) point to the importance of modeling the effects of turbulence level and length scale on pre-transitional boundary layers. However, the authors assume that the integral quantities of quasi-laminar boundary layers are the same as the equivalent purely laminar ( $Tu=0$ ) boundary layer. It will be demonstrated that this assumption is not consistent with experimental data. Sharma et al. (1988) reviewed experimental evidence that turbulence from upstream rows imparts a significant influence on the pre-transitional boundary layers on turbine airfoils. Additionally, the importance of capturing the effects of freestream turbulence on laminar boundary layers has been identified in experimental studies of laminar heat transfer rates by Ames (1995) and Van Fossen et al. (1994).

The phenomenon of a quasi-laminar boundary layer is demonstrated in the cascade heat transfer data of Arts et al. (1990). Figure 3 is a plot of measured heat transfer distributions from Arts et al. (1990) with nominal inlet freestream turbulence levels of 1% and 6%. Additional flow conditions for both data sets in Figure 3 were  $Re_c=1 \times 10^6$  and  $M_{exit}=0.77$ , where  $Re_c$  is Reynolds number based on true chord. Heat transfer augmentations in the leading-edge and pressure-side regions of the airfoil of up to approximately 50% are evident. Given that the only difference between the two experiments is the turbulence level, the enhanced energy transfer across the quasi-laminar boundary layer in the high  $Tu$  case must be primarily due to the penetration of freestream turbulence into the laminar boundary layer.

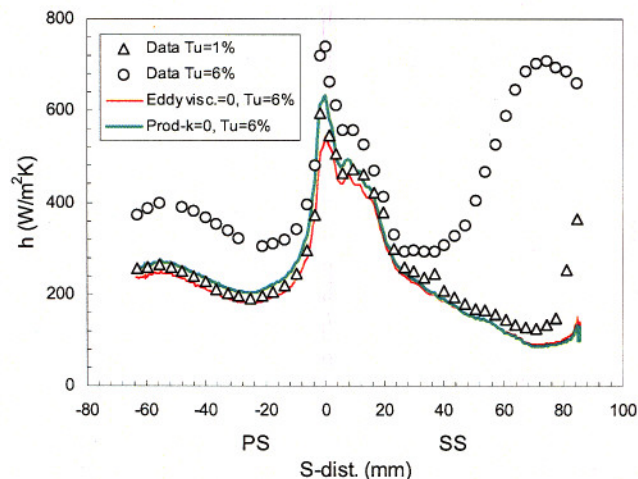


Figure 3. Measured convective heat transfer coefficient distributions from Arts et al. (1990) and CFD predictions run with fully laminar boundary layers.

The data from Arts et al. (1990) was employed to assess various methods for modeling quasi-laminar boundary layers. Uniform surface-temperature conditions were held for each of the simulations consistently with the measured values. CFD simulations (Figure 3) were run fully laminar on both the suction- and pressure-sides of the



airfoil employing common modifications from literature to simulate laminar regions. One such technique tested that is commonly employed in transitional RANS simulations involves setting the eddy-viscosity,  $\mu_t$ , from the turbulence model to zero within the boundary layer. Also tested was the technique reported by Schmidt and Patankar (1988) in which the production term in the  $k$  equation is set to zero in laminar regions.

The heat transfer distribution predicted by setting the eddy viscosity equal to zero with  $Tu=6\%$  is shown in Figure 3. The results for this simulation duplicate the convective heat-load distribution from a purely laminar simulation (not shown). Results from setting the production of  $k$  equal to zero with  $Tu=6\%$ , shown in Figure 3, indicate only a slight increase in the predicted heat-load levels around the airfoil compared to the prediction with  $\mu_t=0$ . From these simulations it is concluded that neither method for modeling laminar flow with elevated freestream turbulence accurately predicts the wall gradients of the quasi-laminar boundary layer.

A model was developed based on studies performed with the data of Arts et al. (1990). Results based on the current model for quasi-laminar boundary layers, labeled as "QL model" (Praisner and Rangwala, 2001), are shown in Figure 4. As seen in this figure, the results from the QL model are more accurate in quasi-laminar regions than the results shown in Figure 3. The current method is based on physical reasoning which links the production terms in the  $k$  and  $\omega$  equations to the concept of self-sustaining turbulence in turbulent boundary layers. The analogy is drawn that in laminar regions of the boundary layer, where disturbances are damped by the mean velocity profile, the production of both  $k$  and  $\omega$  should be negligible. Implicit in this analogy is that the eddy viscosity in a quasi-laminar boundary layer is independent of the mean strain. Minimizing the production terms in the  $k$  and  $\omega$  equations, in contrast to setting  $\mu_t=0$ , allows for the convection and diffusion of freestream turbulence into quasi-laminar boundary layers. For the length scales (i.e. dissipation rates) and turbulence intensities present in the data of Arts et al. (1990), the QL model captures convective heat loads to within  $\pm 10\%$  in quasi-laminar regions for all conditions reported.

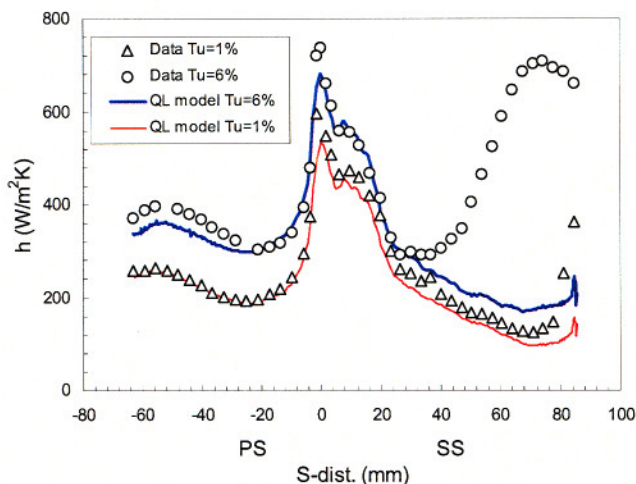


Figure 4. Results from CFD simulations run with the QL model for capturing pre-transitional quasi-laminar boundary layers.

Additional testing of the QL model was performed with the cascade data of Ames (1994) with similar accuracy for convective heat loads for levels of  $Tu$  up to 12% from a simulated combustor (Praisner et al, 2003). Additionally, predictions of stagnation-point heat transfer levels from the QL model are within  $\pm 10\%$  of the correlation of Van Fossen et al. (1994) for a wide range of turbomachinery-specific turbulence and dissipation levels.

To verify that the quasi-laminar boundary layer *shape* is also modeled accurately by the QL model, a validation study was performed with the favorable pressure-gradient, flat-plate data of Blair (1981). Figure 5 is a plot of non-dimensionalized velocity and temperature profiles in the quasi-laminar flow region immediately upstream of transition onset with  $K=0.2 \times 10^{-6}$  and  $Tu=3\%$  nominally, where  $K$  is the acceleration parameter. Also shown are results from CFD predictions performed with the laminar regions simulated by setting  $\mu_t = 0$  (purely laminar) and the QL model. Both the momentum and thermal boundary layer shapes are closely matched with the QL model as compared to the method of setting  $\mu_t = 0$ . Also, the accuracy of the predicted convective heat transfer levels within the quasi-laminar region were as accurately captured as those in the benchmarking against the data of Arts et al. (1990).

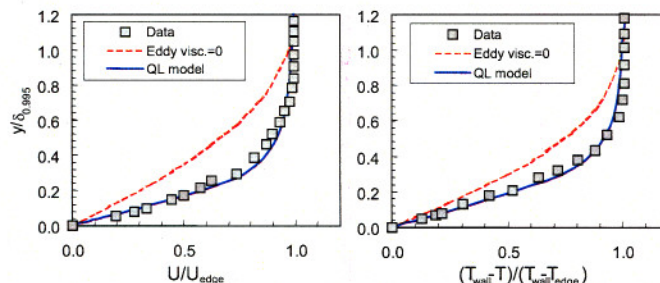


Figure 5. Non-dimensional momentum and thermal boundary layer profiles in a quasi-laminar boundary layer just prior to transition. Data is from Blair (1981).

For the momentum boundary layer shown in Figure 5 the predicted values of momentum-thickness Reynolds number,  $Re_\theta$ , are 23% and 6% below the measured value for the  $\mu_t=0$  technique and QL model respectively. In turn, the shape factors predicted with the  $\mu_t=0$  technique and QL models are 21% and 3% above the measured level of 2.57, respectively. Also, the approximate location of transition onset for the case with  $Tu=6\%$  in Figure 4 is at  $s=28\text{mm}$  on the suction side. The QL-model predicted values of  $Re_\theta$  for this streamwise location differ by 15% between the two turbulence levels considered. These results, taken together with the flat-plate results for  $Re_\theta$ , indicate that any form of modeling that does not accurately capture the turbulence-enhanced transfer characteristics of quasi-laminar boundary layers, will provide inaccurate quantities for transition onset prediction.

Additionally, if one assumes the  $Re_\theta$  value for the  $\mu_t=0$  technique is essentially an exact numerical solution for a condition with  $Tu=0\%$ , these results are in contrast with the assumption made by Roach and Brierley (2000) that integral quantities of pre-transitional boundary layers are unaffected by freestream turbulence. The aforementioned authors supported their assumption by referencing turbulent boundary layer data with elevated  $Tu$  levels. Since turbulence levels within turbulent boundary layers are of the order 10-15% with low freestream  $Tu$ , it is not surprising that they are not appreciably affected by elevated levels of freestream turbulence. In contrast, the low levels of



turbulence present in laminar boundary layers means they are susceptible to significant momentum- and heat-transfer enhancement with the addition of turbulence convected and diffused from the freestream. The results reported here are consistent with the apparent increases in measured  $Re_\theta$  values that may be as high as 30% in pre-transitional boundary layers subjected to elevated levels of  $Tu$  measured by Yaras (2002).

It was found that the effects of roughness on pre-transitional boundary layers were not accurately captured with the combination of the QL model and the modified wall boundary condition for  $\omega$  from Wilcox (1998) for rough walls. This is not surprising considering that the formulation of Wilcox's modification was specific to turbulent boundary layers. However, the assumption of admissible roughness is typically valid for all but the high-pressure turbine in large commercial and military engines. However, in the case of small-scale engines, such as those used for unmanned aircraft, the surface roughness levels from cast airfoils may play an important role in the transition process. Resolution of pre-transitional boundary layers subjected to significant levels of roughness is a topic that requires more attention.

Results obtained with the QL model for various values of turbulent Prandtl number,  $Pr_T$ , show little variation in boundary layer qualities. Variation of  $Pr_T$  from a molecular level of 0.7 to a turbulent level of 0.9 resulted in variations in predicted heat flux and skin-friction levels of less than 5 percent in quasi-laminar regions. This may be related to the fact that turbulent mixing in quasi-laminar boundary layers is significantly lower than in turbulent boundary layers. While not comprehensively validated, it appears that there may be no need to employ different turbulent Prandtl numbers for laminar and turbulent regions of the flowfield in simulations that employ the QL model.

## MODELING ATTACHED-FLOW TRANSITION

Having demonstrated an ability to capture the development of freestream turbulence level and dissipation rate as well as pre-transitional quasi-laminar boundary layer details, a database of experimental test cases was constructed to evaluate methods for transition onset prediction. The construction involved performing laminar simulations of experimental test configurations with appropriate freestream and wall boundary conditions. Inlet levels of turbulence and dissipation rate were set employing the aforementioned techniques for matching the decay rate of  $Tu$ . The  $k-\omega$ -based QL model for capturing the pre-transitional boundary layers was employed as well. For each experimental case considered, the measured and predicted static-pressure distributions were in close agreement. Transition onset was considered to occur in the data sets where wall-gradient quantities first began to deviate from fully laminar simulations. Only cascade geometries of turbomachinery-specific airfoils were considered, and both open-literature and in-house data were used to build the database of 57 cases. The 57 cases themselves consisted of seven different geometries tested in experiments with various boundary conditions.

The database does not necessarily represent accurate physical quantities, but instead represents the best available estimates of flow quantities that can be provided by two-equation turbulence model-based RANS simulations. The primary use of the database was to determine if, given accurate freestream turbulence and pre-transitional boundary layer modeling, accurate transition-onset predictions could be obtained with RANS simulations across a broad range of flow conditions and geometries.

## A Review of Models for the Onset of Transition

The most successful physical model for the transition process is that due to Emmons (1951), Schubauer and Klebanoff (1955), and Narasimha (1957). In this model, transition is considered to be the result of the random formation of "spots" of turbulence in the boundary layer over some finite region in the streamwise direction. These turbulent spots grow as they convect downstream, and the intermittency (i.e. the fraction of time the flow is turbulent) increases in the streamwise direction until the entire surface is covered with them. At that point, the boundary layer is considered fully turbulent.

The foregoing would suggest that an assessment of the effects of various flowfield parameters on transition must be an evaluation of the way in which they affect the formation and subsequent growth of turbulent spots and/or wake-induced turbulent strips. Several authors have conducted experimental studies in that regard (e.g. Clark et al., 1994, Gostelow et al., 1994, and Halstead et al., 1997), and others (e.g. Chen and Thyson, 1971, Dey and Narasimha, 1990, and Solomon et al., 1996) have incorporated information on turbulent-spot formation and kinematics into integral methods for calculating intermittency and, by extension through a "linear combination model" after Dhawan and Narasimha (1958), skin friction. Still others (e.g. Suzen and Huang, 2000 and Steelant and Dick, 2001) have made use of the "universal" intermittency distribution to derive transport equations for intermittency that are solved alongside the RANS equations or used some combination of the correlations of Abu-Ghannam and Shaw (1980), Drela (1995), and Solomon et al. (1996) to evaluate intermittency (e.g. Gier et al., 2000, Thermann et al., 2001, Roux et al., 2002, and Roberts and Yaras, 2003) through transition. Subsequently, some of the same authors modified the calculated eddy viscosity according to the fraction of time the flow is predicted to be turbulent through the transition zone. As previously stated, pre-transitional boundary layers with elevated  $Tu$  levels may not be adequately modeled by setting  $\mu_T$  equal to zero upstream of transition onset.

The review article of Mayle (1991) spurred renewed interest in the ideas of Emmons (1951) and Narasimha (1957) for the prediction of transition in turbomachines, and much of the recent work described above followed recommendations from that paper closely. In particular, the concept of the "universal" intermittency distribution as described in detail by Narasimha (1985) has been used to build correlations for transition onset (Mayle, 1991), turbulent-spot generation rates (Fraser et al., 1994, Gostelow et al., 1994), and transition length (Fraser et al., 1994, Gostelow et al., 1994).

At the root of many correlations used to predict transition onset is the  $F(\gamma)$  technique of Narasimha (1985), whereby measured streamwise variations of intermittency,  $\gamma$ , are plotted in the form

$$F(\gamma) = [-\ln(1-\gamma)]^{1/2} \quad (6)$$

Narasimha (1957) proposed that all turbulent spots are formed randomly in time and spanwise location at a single streamwise station in the flow. Under that hypothesis, which is now known generally as "concentrated breakdown," Equation 6 becomes

$$F(\gamma) = \left( \frac{n\sigma}{U_\infty} \right)^{1/2} (x - x_t) \quad (7)$$

for constant-velocity flow along a flat plate. In equation 7,  $x_t$  is the streamwise location where all spots are formed,  $n$  is the number of spots formed at that position per unit time and per unit spanwise distance,  $U_\infty$  is the freestream velocity,  $\sigma$  is Emmons (1951) non-dimensional spot-propagation parameter, and  $x$  is a location on the flat-plate surface further downstream than  $x_t$ .



Dhawan and Narasimha (1958) also showed that variations of intermittency through the transition zone possess a high degree of similarity if the streamwise distance is suitably non-dimensionalized. They demonstrated that the transitional intermittency-variations from a number of experiments collapsed on a single curve when the streamwise distance was represented by

$$\xi = \frac{x - x_t}{x_{75} - x_{25}} \quad (8)$$

where  $x_{75}$  and  $x_{25}$  are the streamwise positions where the intermittency is 0.75 and 0.25, respectively. The same authors also showed that the available intermittency data were well represented by the equation

$$\gamma = 1 - e^{-0.412 \xi^2} \quad (9)$$

Equation 9 has become known as the "universal" intermittency-distribution (Narasimha, 1990 and Narasimha, 1991). Like Equation 7, Equation 9 is a consequence of the assumption of concentrated breakdown as applied to the transition model of Emmons (1951) in constant velocity, flat-plate flow.

Many authors have shown that it is possible to linearize intermittency distributions using Equations 6 and 7 and, consequently, to plot the data in the universal form of Equation 9 (e.g. Owen, 1970). This is true even under conditions of changing pressure gradient and/or freestream velocity (Sharma et al., 1982, Gostelow et al., 1994, Fraser et al., 1994). As an illustration of this phenomenon, representative data from Clark (1993) are plotted in Figure 6. Experimental intermittency distributions for flat-plate flows under both favorable and adverse pressure gradient conditions are plotted, and both agree with the universal curve very well. This is surprising in the case with the favorable pressure gradient since the local velocity varies by a factor of more than 6.7 over the streamwise distance represented in the figure. Note that both the spot shape parameter and the freestream velocity itself are considered constant and brought outside an integrand in the derivation of equation 7, and neither of these assumptions is valid in the experiment of Clark (1993). Intermittency variations predicted with a time-marching simulation of the transition zone like that described by Narasimha (2003) are also plotted in Figure 6. These predicted intermittency distributions are taken along the centerline of a flat-plate flow at Mach 0.5. Spot propagation parameters were as measured by Clark et al. (1994), and three different distribution functions for spot generation were considered. The universal curve fits the predicted intermittency distributions very well, not just when concentrated breakdown prevails, but also for both a bivariate normal (in streamwise and spanwise directions) spot generation function and a point source located off the plate centerline.

Observations like those presented here with respect to the universal curve are not new (See, e.g. Dhawan and Narasimha, 1958). In more recent times Mayle (1991) used the  $F(\gamma)$  technique to develop a correlation for transition onset, where onset was taken to be the x-intercept of the  $F(\gamma)$  plot. Also, correlations for length as well as turbulent-spot generation rates under a variety of flow conditions (Mayle, 1991, Gostelow et al. (1994), and Fraser et al., 1994) have been derived. From the discussion above, it does not follow that if it is possible to linearize experimental data by plotting  $F(\gamma)$ , then the transition is consistent with a flat-plate flow undergoing transition via a concentrated breakdown of the laminar boundary layer. When the current database for attached-flow transition onset is compared to one such correlation from Mayle (1991), as in Figure 7, there is considerable scatter. Testing against the database revealed a success rate of approximately 50% in predicting onset within 10% of the measured location in terms of surface distance. Also, transition onset typically occurs at lower Reynolds numbers than predicted by the Mayle (1991)

relation. Similar results to those in Figure 7 are reported by Simon and Ashpis (1996) for comparisons made between data and the Mayle (1991) correlation. In light of these findings, it might be better to develop correlations for transition onset and turbulent-spot production rates, for example, from direct measurements like those first reported by Hofeldt (1996). Such direct measurements are difficult, however, and little data is available at present to create such correlations.

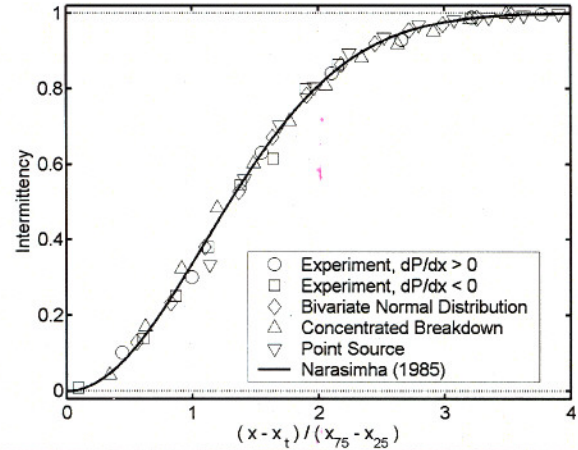


Figure 6. A comparison between the "universal" curve of Narasimha (1985) and both experimental data and simulations from Clark (1993).

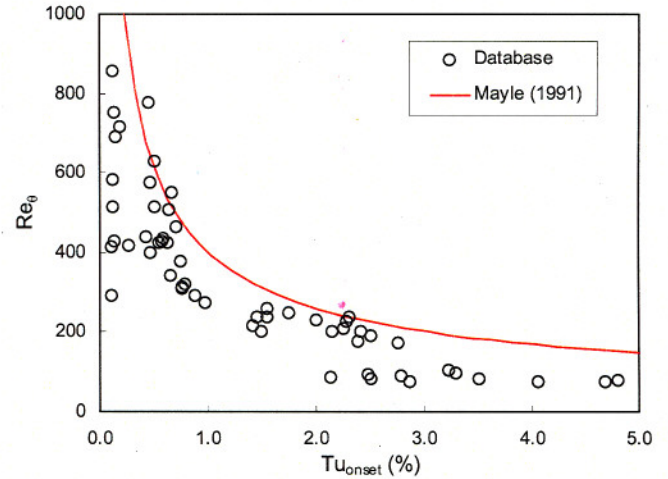


Figure 7. A comparison between the current database for attached-flow transition onset and the correlation of Mayle (1991).

Both Tani (1969) and Reshotko (1976) review a number of models that are not based on the concept of universal intermittency, and they both point out that one of the first was due to Liepmann (1945). Many authors refer to Liepmann (1943) as the source of this idea, but the 1945 publication is the correct one. Liepmann supposed that transition onset occurs when the local Reynolds stress in the perturbed laminar boundary layer equals the local friction velocity. Liepmann's idea has been recast



and used by others. For example, Van Driest and Blumer (1963) correlated the local vorticity Reynolds number, which like the friction velocity depends on the normal gradient of streamwise velocity in 2D flow, at transition onset with freestream turbulence and pressure gradient. Recently, Mayle and Schulz (1997) referred to the formulation of Liepmann's criterion due to Sharma et al. (1982) as appropriate for transition onset. Sharma et al. (1982) argued that the local Reynolds stress itself depends on the local root mean square of streamwise velocity perturbations and stated that transition onset occurs when

$$\frac{u'}{u_*} = 3.0 \quad (10)$$

based on experimental data related to a turbine airfoil suction-side flowfield. In equation 10,  $u_*$  is the local friction velocity and  $u'$  is the fluctuating component of the local streamwise velocity. Liepmann (1945) argued the same case based on his own experimental data. Following Liepmann's analysis and re-casting his correlation in the form of equation 10 results in a constant on the right hand side equal to 7.5 rather than 3. In addition, Roach and Brierley (2000) report that the constant in equation 10 varies from 3.0 to 7.4 for the ERCOFTAC T3 test cases.

If one assumes that  $u'$  within the quasi-laminar boundary layer is modeled to a reasonable level of accuracy with the QL model, it might be possible to predict transition onset based on a relation like that in Equation 10. In Figure 8 the quantity  $u' / u_*$ , evaluated at transition onset, is plotted for all cases in the current database. For comparison both the constants of Sharma et al. (1982) and Liepmann (1945) are also plotted. Transition onset seems to occur at much lower levels of  $u' / u_*$  than those indicated by Sharma et al. (1982) and Liepmann (1945) over the entire database.

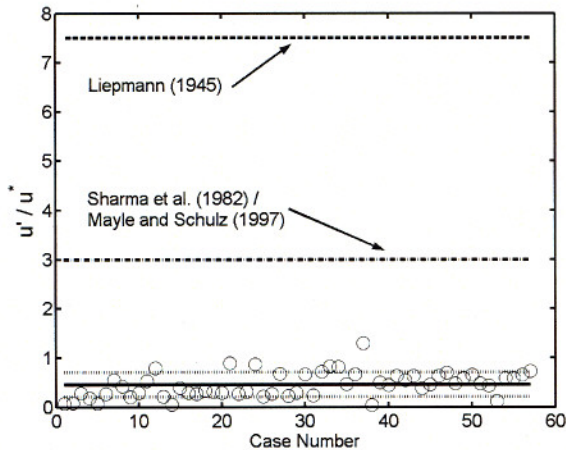


Figure 8. A comparison between the transition onset criteria of Liepmann (1945), Sharma et al. (1982), and Mayle and Schulz (1997) and the current attached-flow database.

The poor correlation of the database in Figure 8 may likely be a result of the assumption of isotropic turbulence within the quasi-laminar boundary layer inherent in the QL model. Also, one notes that the studies of Sharma et al. (1982) and Liepmann (1945) pre-date the use of conditional sampling techniques for boundary-layer measurements (See, e.g., Suder et al., 1988 and Kim et al., 1994). So, it could be that the local rms of velocity fluctuations in the boundary layer was largely influenced by the passage of turbulent spots over the fixed hot wires in the experiments of both Liepmann (1945) and Sharma et al. (1982). As such, the criteria represented by equation 10 might be more indicative of

turbulent-spot detection than of the state of a quasi-laminar boundary layer at transition onset. The foregoing argument is supported by the results of a simple calculation. Consider a boundary layer profile undergoing transition to be a linear combination of laminar and fully turbulent profiles weighted on the intermittency, as suggested first by Dhawan and Narasimha (1958), and let onset occur in a Blasius boundary layer on a flat plate at a local streamwise Reynolds number of 250,000. If one represents the turbulent profiles by a  $1/7^{\text{th}}$  power law and presumes there is no change in boundary layer thickness at transition onset (strictly speaking, there can be no change in the local momentum thickness), then at  $y^+ = 25$ , the local rms becomes about 3 times the local friction velocity if the intermittency is 10%. This is very much in keeping with the results of Sharma et al. (1982). In any regard, the results shown in Figure 8 suggest that even with the current modeling of pre-transitional boundary layers, accurate RANS-based transition predictions can not be obtained with a model of the type in Equation 10.

A correlation for transition onset that was developed independently of the concept of intermittency is due to Abu-Ghannam and Shaw (1980). Their work was recast by Drela (1995) using the boundary layer shape factor as a correlating parameter and collectively these relations were used by a number of others (e.g. Fraser et al., 1994, Gier et al., 2000, and Roux et al., 2002). Abu-Ghannam and Shaw (1980) measured the time-mean near-wall streamwise velocity with a hot wire, and they determined the start of transition to occur where that parameter began to deviate from the reference laminar level. As such, their method is consistent with demarcating transition start by an increase in the local skin friction over the laminar level, and that is in essence the technique used to determine onset for the current database. The percent difference between the momentum-thickness Reynolds number predicted with the correlations of Abu-Ghannam and Shaw (1980) and the actual values found in the current database is plotted in Figure 9. It was found that the correlation of Abu-Ghannam and Shaw (1980) produces errors in the momentum-thickness Reynolds number in excess of 20% in 39 of the 57 cases in the database. Testing against the database revealed a success rate of approximately 68% in predicting onset within 10% of the measured location in terms of surface distance. Testing of the correlation utilizing inlet turbulence levels instead of local levels, which is consistent with the original formulation of the model, did not improve the correlation of the database.

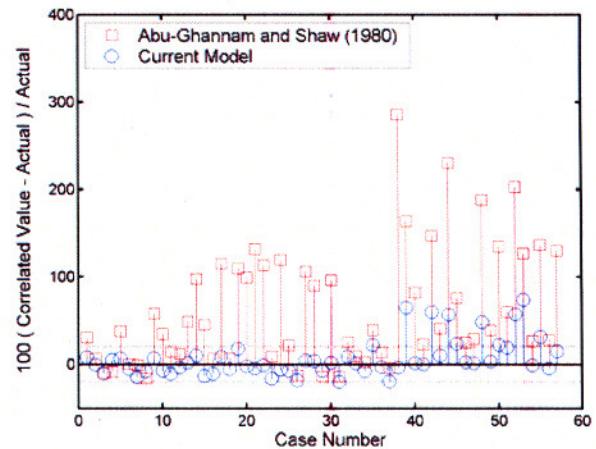


Figure 9. A comparison of the efficacy of the current transition-onset model for attached-flow with that of Abu-Ghannam and Shaw (1980).



### A Review of Models for Transition Length

Early in the course of this work, three separate transition-length correlations were evaluated in conjunction with the onset model of Abu-Ghannam and Shaw (1980) to predict the development of intermittency through transition for flowfields in the current database. These were the models of Gostelow et al. (1994), Fraser et al. (1994), and Solomon et al. (1996). However, the modeling of transition length was eventually discarded, and abrupt trips at onset were used exclusively in this effort. This decision was made for a number of reasons. First, the present authors thought it was inadvisable to stack any correlation for length upon another correlation for transition onset since each relation must have its own attendant uncertainty. Further, the models of Gostelow et al. (1994) and Fraser et al. (1994) each assume that transition length is a function simply of the freestream turbulence intensity and the pressure gradient parameter at onset. Because onset on a turbine airfoil often occurs in a region where the pressure gradient changes sign, neither length model was found acceptable. So, the model of Solomon et al. (1996), which considers the local effects of pressure gradient on turbulent spot growth in the determination of the transition length, was tested. Although that model was expected to perform better on turbine airfoils and did so, the predictive capability of the relation was still lacking. Moreover, it was noted that all three length models depended on correlations for turbulent-spot production rates that were derived from experimental data using the  $F(\gamma)$  technique. On account of the discussion presented above relative to the  $F(\gamma)$  technique, none of these models were adopted. Finally, the implementation of a transition-length model requires that a streamline-based application of the modeling be implemented. That is, it becomes necessary to track particles from transition onset through 3D flowfields along airfoil surfaces. So, without the use of an intermittency-transport equation (Suzen and Huang, 2000), such a model implementation becomes very cumbersome.

Again, based on the difficulties and inaccuracies inherent in transition-length modeling, it was decided only to model transition onset and to use simple instantaneous (i.e. abrupt) trips. Since an abrupt trip implies the sudden increase in turbulence production in the context of this work, and because there is some finite distance over which the boundary layer and turbulence model respond to that, a finite transition length is obtained in practice (Praisner et al., 2003).

### A New Model for Attached-Flow Transition

Morkovin (1978) coined the term bypass transition, and has alerted designers to the implications of such phenomena many times. In his NATO AGARDograph he stated that designers must become "rather sensitive to bypasses when transition risks imply risks to the basic mission of the design." Such a situation obtains in axial flow turbomachinery both in the compressor and turbine modules. Morkovin also pointed out that "it is easy to criticize; it is another matter to offer a constructive suggestion to the designer." With these ideas in mind and with the current capability to predict local flow features at the onset of transition for experiments pertinent to turbomachinery design, the database was analyzed to build a new model for attached-flow transition onset.

It was postulated that the boundary-layer momentum thickness at the onset of transition ( $\theta$ ) depends upon a number of local flow variables at the edge of the boundary layer and the local wall temperature ( $T_w$ ). These flow variables were taken to include the density ( $\rho$ ), the dynamic viscosity ( $\mu$ ), the sonic speed ( $a$ ), the driving temperature for heat transfer ( $T_g$ ), the thermal conductivity of the fluid ( $k$ ), the specific heat at constant pressure ( $c_p$ ), the magnitude of the flow velocity ( $U_\infty$ ), the streamwise velocity gradient ( $dU_\infty/ds$ ), the

root-mean-square of streamwise velocity fluctuations ( $u'$ ), and their length scale ( $\lambda$ ).

Applying the Buckingham-Pi Theorem via the "step-by-step" technique of Massey (1986), it is possible to represent the physical process as a function of 7 non-dimensional parameters. The relation is

$$Re_\theta = f(M, T_g/T_w, K, Tu, Pr, \lambda/\theta) \quad (11)$$

The non-dimensional parameters in equation 11 are the momentum-thickness Reynolds number at transition onset ( $Re_\theta$ ), the Mach number ( $M$ ), the gas-to-wall temperature ratio ( $T_g/T_w$ ), the acceleration parameter ( $K$ ), the local turbulence intensity ( $Tu$ ), the molecular Prandtl number ( $Pr$ ), and the ratio of turbulent length scale to momentum thickness ( $\lambda/\theta$ ). Note that the physical dimensions used to define the indicial matrix are mass ( $m$ ), length ( $L$ ), time ( $t$ ), temperature ( $T$ ), and heat ( $H$ ). Because heat is invoked as a dimension, it is assumed that there is no substantial conversion of mechanical energy into thermal energy. So, the results are restricted to flows of gases with moderately supersonic Mach numbers, but this is not a limitation for the gas-turbine situation.

The non-dimensional parameters in Equation 11 were tabulated for each case in the database, and the results were correlated to determine the combination of non-dimensional parameters that provided the best collapse of the data. The best correlation for transition onset was found when

$$Re_\theta = A \left( Tu \frac{\theta}{\lambda} \right)^B \quad (12)$$

where  $A$  and  $B$  are constants equal to 8.52 and -0.956, respectively. The entire database is plotted in Figure 10. Equation 12 implies that the local momentum thickness at transition onset is a function of only one non-dimensional parameter that is a product of two of the basic non-dimensional parameters derived directly from the "step-by-step" method of Massey (1986).

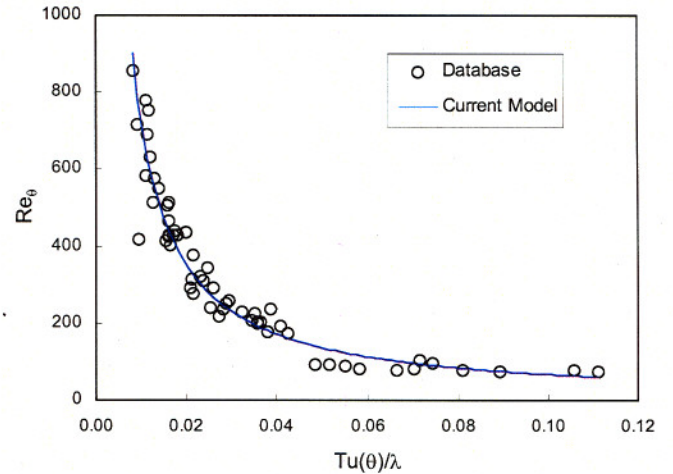


Figure 10. The current model for the onset of attached-flow transition compared to the database.

An ability to determine the edge of the boundary layer in a robust manner is an important aspect of transition modeling techniques based on integral and edge quantities. The edge of the boundary layer was taken to be the distance from the wall at which the local vorticity dropped to 1% of the maximum value in the O-grid at that streamwise



grid location. This method, reported by Michelassi et al. (1998), provides a robust and accurate edge detection technique for laminar boundary layers. Variations in the percentage of the maximum vorticity used to define the boundary layer edge between 0.8% and 1.8% resulted in variations in the coefficient of correlation of the least-squares fit for Equation 12 of between 0.95 and 0.96. The boundary layer grid densities outlined in the Computational Methods section were necessary for the implementation of the vorticity-based edge detection method.

As seen in table 1, all the non-dimensional parameters, save the molecular Prandtl number, varied markedly at transition onset over this database. For example, transition onset occurred under both favorable and adverse pressure gradients. The strength of the pressure gradients covers the range from above relaminarization ( $K > 3 \times 10^{-6}$ ) on the favorable side through Thwaite's separation criterion ( $K Re_\theta^2 < -0.09$ , See White, 1991) under decelerating conditions. Both adiabatic flows and those with velocity profiles that were affected by the temperature dependence of viscosity were part of the database. Also, the range of Mach numbers covered incompressible through transonic flows. The local turbulence intensity varied by two orders of magnitude, and while the maximum value may at first consideration seem low, one must remember that the inlet turbulence intensity was much higher. Further, the ratio of local turbulence length scale to momentum thickness at onset varied by an order of magnitude. Again, the molecular Prandtl number was essentially constant for all points in the database.

Table 1: Variation of non-dimensional parameters at transition onset.

Variable	Range
$Re_\theta$	73 - 856
$K \times 10^6$	-1.9 - 4.8
$K Re_\theta^2$	-0.15 - 0.057
$M$	0.05 - 1.24
$T_g / T_w$	1.0 - 1.41
$Tu_{onset} (\%)$	0.11 - 5.09
$\lambda / \theta$	4.26 - 66.2
$Pr$	0.71 - 0.71

### Physical Significance of the Current Attached-Flow Model

Equation 12 was incorporated into the airfoil design system directly with the factor and power in the equation set equal to 8.52 and -0.956, respectively. However, it is possible to recast the relation in such a way that gives insight into its physical significance. One notes that the constant  $B$  in the relation is very close to -1. If that value is accepted, then, after some algebraic manipulation, Equation 12 becomes

$$100 \left( \frac{u'}{\lambda} \right) \left( \frac{\rho \theta^2}{\mu} \right) = A_1 \quad (13)$$

where  $A_1$  is another constant that may be evaluated directly as the mean of values occurring at transition onset in the database. Here,  $A_1$  was found to be  $7.0 \pm 1.1$ . Note that Equation 13 implies that transition onset occurs when the ratio of a boundary-layer diffusion time ( $\rho \theta^2 / \mu$ ) to a timescale associated with the large-eddy turbulent fluctuations ( $t_e = \lambda / u'$ ) becomes a critical value.

It is instructive to consider the implications of Equation 13 for a Blasius boundary layer undergoing transition. The usual form of the laminar diffusion timescale,  $t_{db}$  is  $\rho \delta^2 / \mu$  (See e.g., Schlichting, 1979, and Hofeldt et al., 1998) where  $\delta$  is the thickness where the local velocity becomes 99% of the freestream value and  $\rho$  is the fluid density. The ratio of 99% velocity thickness to momentum thickness

in a Blasius boundary layer is 5:0.664. Substituting into Equation 13, taking  $A_1$  equal to 7.0, and rearranging gives

$$t_e = 0.25 t_d \quad (14)$$

The time for a Blasius boundary layer to grow to a thickness  $\delta$  is  $1/25^{\text{th}}$  the laminar diffusion timescale (Schlichting, 1979). So, transition onset would occur for the Blasius boundary layer when the local eddy timescale approached a level associated with a growth of  $\approx 6$  boundary layer thicknesses. Schlichting (1979) gives the smallest unstable wavelength of a Blasius boundary layer as  $\approx 6\delta$ . So, Equation 14 implies that the onset of bypass transition occurs when the local eddy timescale reaches a timescale associated with the wavelength of a Tollmien-Schlichting (TS) wave.

Although one typically does not associate TS activity with bypass transition, it has been noted by Herbert (1988) that the ultimate breakdown associated with the appearance of "spikes" in hot-wire records and the first formation of turbulent spots in natural transition occurs over a length scale of about 1 TS wavelength. Also, Walker and Gostelow (1990) have measured frequencies consistent with TS activity in boundary layers undergoing bypass transition in adverse pressure gradients. Additionally, Mack (1975) noted that often TS frequencies persist in boundary layers undergoing natural transition beyond the range of applicability of small disturbance theory. Volino (2002) also reported that for separated-flow transition, TS frequencies were detected for both low and high levels of  $Tu$ . So perhaps the results of this exercise are not so surprising. Again, the real implication of this discussion is that when the ratio of the turbulent-eddy time scale to the laminar diffusion time reaches a critical value, bypass transition occurs. Further, the critical value of this ratio is nearly constant over a range of flow conditions consistent with gas-turbine engines.

### MODELING LAMINAR SEPARATION AND TURBULENT REATTACHMENT

"Of all the transition modes, there is none more crucial to compressor and low-pressure turbine design and none more neglected than separated-flow transition" (Mayle, 1991). As attempts are made to reduce airfoil counts, and hence component cost and weight, airfoil loadings need to increase. Highly loaded airfoils are more prone to experiencing laminar separations (Figure 11) and stall. In the stalled condition profile losses can increase as much as 500% over the case where the separation reattaches to the airfoil. Laminar separations occur in the leading-edge, suction-side regions of compressors and the aft suction-side regions of Low-Pressure Turbine (LPT) airfoils. Airfoil stall causes compressor surge and poor performance of LPTs at cruise conditions.

If the laminar shear layer formed by a separation transitions to a turbulent state close enough (i.e. in a stream-wise sense) to the separation location, it typically reattaches to the airfoil surface as a result of turbulent mixing that entrains high-momentum fluid into the near-wall region. This scenario is schematically depicted in Figure 11a. However, if transition of the shear layer occurs sufficiently far downstream of separation, the layer typically does not reattach, resulting in a stalled condition as shown in Figure 11b. It is therefore critical that a design system be capable of predicting the existence of a laminar separation and whether or not the laminar separation will reattach.



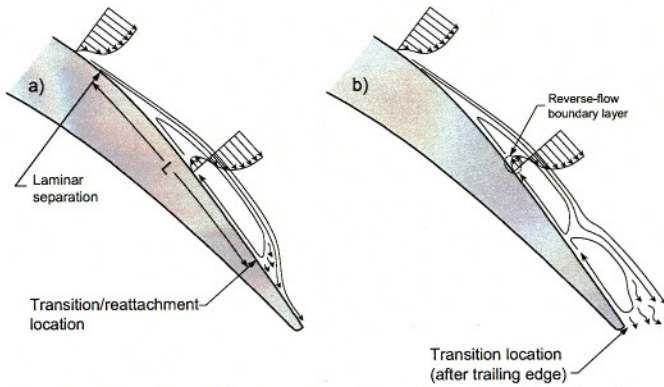


Figure 11. Schematic representation of suction-side, laminar-separation characteristics showing both reattached (a) and stalled (b) conditions.

As a first step in developing a transition modeling capability for separated flow, a proof-of-concept study was executed with the goal of determining if a separated-flow transition model could be effectively implemented in a RANS code. For this study, CFD simulations of cascade experiments were run with imposed point-like trips set according to experimental hot-film data. Figure 12 is a plot of separation and reattachment locations as a function of exit Reynolds number for a cascade airfoil with  $Tu=5\%$  (data if from Butler et al., 1988). The total suction-side surface length of the airfoil for this case was 37.1 mm. Experimental and computational results are shown.

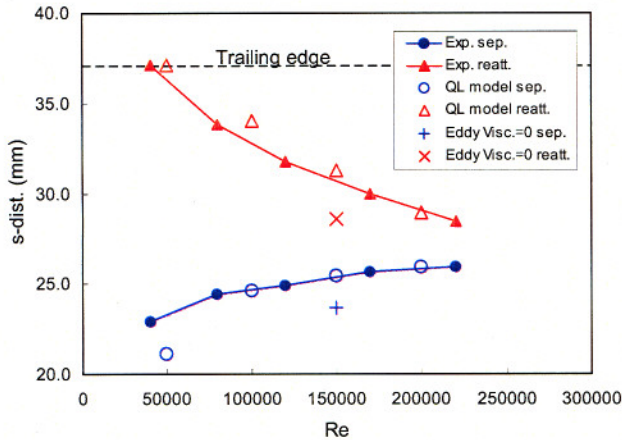


Figure 12. Measured and predicted separation and reattachment locations. Transition was specified in the simulations based on data.

It can be seen in Figure 12 that the separation and reattachment locations from simulations utilizing the QL model for the pre-transitional boundary layers are in close agreement with the data. The deviation from the data at the lowest Reynolds number was a result of stall occurring in the simulation and subsequent unsteadiness of the separation location. For a Reynolds number of  $1.5 \times 10^6$  a simulation was also run with the turbulent viscosity set to zero in laminar regions and the results are also plotted in Figure 12. For this simulation the separation location occurs upstream of the measured location. This is consistent with the quasi-laminar boundary layer shape, and hence

near-wall momentum, not being accurately modeled by setting  $\mu_T=0$ . Similar comparisons were made with additional cascade data at a variety of turbulence levels and the results were consistent with those in Figure 12. The calculated loss levels from the simulations shown in Figure 12 were in very close agreement with the measured values. The conclusion of this study was that the RANS code with abrupt trips and the QL model for pre-transitional/separation boundary layers would provide an accurate framework for separated-flow transition modeling.

So, in addition to the attached-flow transition studies, a CFD-supplemented database of laminar-separations with turbulent-reattachment was constructed based on 47 in-house and open-literature experimental cascade data sets. The test cases for the separated-flow database include laminar separations with turbulent reattachment on both compressor- and turbine-specific geometries. Some of the data sets included in the database are from airfoils on the verge of stall. Like the attached-flow database, the separated-flow database covers a significant range of turbomachinery-specific flow parameters.

### A Review of Models for the Onset of Separated-Flow Transition

One common method for predicting the transition location of a near-wall bounded shear layer involves the use of a correlation that was developed for attached-flow transition such as either the Mayle (1991) or Abu-Ghannam and Shaw (1980) model. These models rely on a non-dimensional boundary layer thickness ( $Re_\theta$  or shape factor) for the prediction of transition onset and were developed with data for attached-flow transition. As depicted in Figure 11, in the separated region, the only attached boundary layer that exists is the reverse-flow boundary layer within the separation bubble. The primary issue with employing an attached-flow transition model in a region where the flow is separated is that the physical significance of  $Re_\theta$  fundamentally changes once the boundary layer separates.

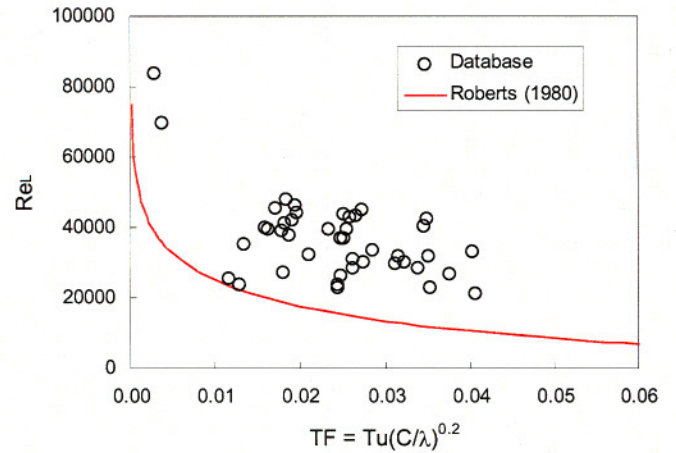


Figure 13. A comparison between the separated-flow transition model of Roberts (1980) and the separated-flow transition database.

A rather unique model for the prediction of separated-flow transition was reported by Roberts (1980), in which the distance from the separation location to the shear layer transition location ( $L$  in Figure 11) is related to freestream turbulence quantities. This model is unique in that it considers both turbulence intensity and length scale in



predicting separated-flow transition onset. Figure 13 is a comparison between predictions performed with the model of Roberts (1980) and the separated-flow database. Plotted in this Figure is Reynolds number based on  $L$  versus the local "Turbulence Factor" which is defined as  $TF = Tu (C/\lambda)^{0.2}$ , where  $C$  is the airfoil chord. The highest level of turbulence factor considered in the development of the Roberts (1980) model was approximately 0.06. This model was developed for external flows with low free-stream turbulence levels ( $<0.2\%$ ). The only database cases that are well correlated by this model are the cases in which  $Tu < 0.6\%$  (Figure 13). The Roberts model (1980) does not correlate database cases with  $Tu > 0.6\%$  well enough for implementation in a design system. Additionally, alteration of the model by leaving out the length scale in the calculation of  $TF$ , as suggested as a possible modification by Roberts (1980), did not improve the correlation of the database.

Other separated-flow transition models have been reported by Walker (1989), Mayle (1991), and Hatman and Wang (1999). These models relate separation length to the conditions of the laminar boundary layer at the separation location. RANS-based simulations employing models of this type have proven to be at least trend accurate in the prediction of separated transition (Volino, 2002, Houtermans et al., 2003). The separated-flow transition database was employed to test the models of Mayle (1991) for "long" and "short" bubbles and a comparison of the predicted and measured bubble lengths is shown in Figure 14. It can be seen in this figure that neither the long- nor the short-bubble model provides sufficient accuracy for design purposes. Similar results were obtained for comparisons between the models due to Walker (1989) and Hatman and Wang (1999) and the separated-flow database. These results are supported by Volino (2002) who reported that the correlations of Hatman and Wang (1999), Mayle (1991), and Davis et al. (1985) give "rough" estimates for the transition behavior of his experimental test cases.

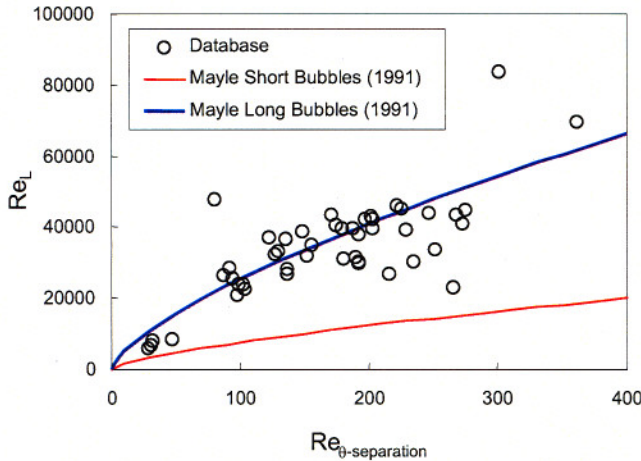


Figure 14. A comparison between the separated-flow transition models of Mayle (1991) and the separated-flow transition database.

#### A New Model for Separated-Flow Transition

In the context of RANS simulations the authors believe that the multi-modal nature of transition is best captured by employing two separate models for attached and separated transition. So, following the body of material concerning models for separated-flow transition summarized above, a new model has been developed based on the

separated-flow database. The same dimensional-analysis technique used for the attached-flow model was employed in the development of this model. The best correlation of the database was obtained when the length of the bubble was related to the state of the boundary layer at separation. The form of the current model is:

$$\frac{L}{S_{sep}} = C Re_{\theta-sep}^D \quad (15)$$

where  $C$  and  $D$  are constants equal to 173.0 and -1.227, respectively,  $L$  is the distance between separation and transition onset and  $S_{sep}$  is the surface distance from the stagnation point to the separation location.

The separated-flow database is shown in Figure 15 in the context of the current transition model. The reasonably good correlation of the database with the recasting of Walker's original idea supports the assertion that for viscously dominated, near-wall bounded separations, the bubble size scales on the state of the boundary layer at separation. While Equation 15 does not explicitly contain turbulence quantities, they are still important in the determination of  $Re_{\theta}$  at the separation location if a model, such as the current QL model, is employed to capture the effects of freestream turbulence on the pre-separation quasi-laminar boundary layer. Additionally, it should be noted that equation 15 was implemented in the design system in a conservative fashion by setting  $C$  at a level 20% higher than the least-squares-fit value plotted on Figure 15 as "current model." This conservatively defined correlation is also plotted in Figure 15 as "shifted model."

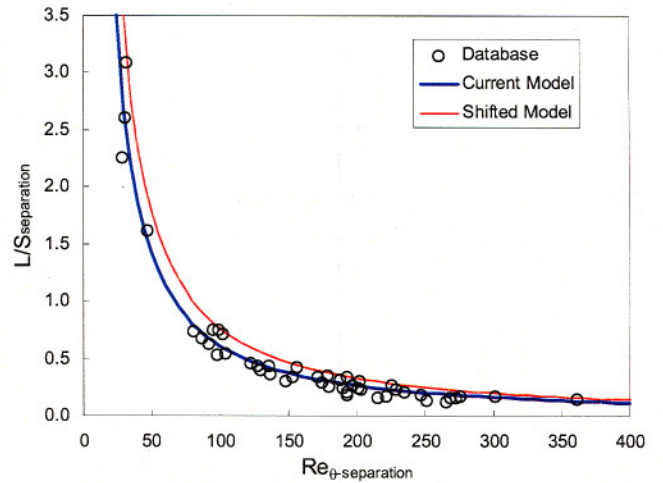


Figure 15. The current model and database for separated-flow transition. The model with a conservative shift is also shown.

In his experimental assessment of the Pack B airfoil, Volino (2002) reported that boundary layer reattachment occurs essentially simultaneously with transition onset for separated flow transition. This supports the assertion made by Lou and Hourmouziadis (2000) that the transition length is very short because the lack of wall damping in the shear layer. Also, Walker et al. (1988) reported that abrupt transition is a relatively (compared to transition-length models for separated flow) realistic model of the transition region in laminar separation bubbles. So, as in the case of attached-flow transition, abrupt transition is assumed for the implementation of the current separated-flow model in the RANS solver. Validation of the many assumptions involved in the development of both models as well as their implementation is reported in Part II of this work.



### Physical Significance of the Current Separated-Flow Model

While the concept of "long" and "short" bubbles has been discussed in literature relating to separated-flow transition for many decades, the present results suggest that the concept may not be important in turbomachinery configurations. The present database is in conflict with reports of Hatman and Wang (1999) and Houtermans et al. (2003) where the existence of two bubble regimes seems evident from data. In the current database, no "long" bubbles, that significantly alter airfoil pressure distributions, were found that also reattached to the airfoil. In other words, separations that do not reattach, and hence alter the turning characteristics and loadings of airfoils, are not referred to as bubbles here as they are not closed. Large reattaching bubbles that significantly alter pressure distributions are possible on flat-plate configurations such as that employed by Hatman and Wang (1999) if reattachment occurs downstream of the simulated trailing edge. Therefore, their correlation may still be useful in predicting where the laminar shear layer transitions downstream of an airfoil trailing edge. The present database shows a continuous distribution of separation behavior up to the point of stall. This is consistent with the results of Houtermans et al. (2003) for their "short" bubble regime. The data regarded as reflecting "long" bubble behavior by Houtermans et al. (2003) is here interpreted as arising from stalled conditions. So, the authors believe that the "short" bubble regime primarily describes separation behavior *with* reattachment. In this work, if separated-flow transition onset is predicted to occur downstream of the airfoil trailing edge, then the airfoil is run fully laminar.

### CONCLUSIONS

The ability to model accurately the development of freestream disturbances has been shown to be an important aspect of any transition modeling capability. Evidence has been presented that the effects of freestream turbulence on pre-transitional boundary layers should be accurately modeled before any form of empiricism is applied for the prediction of transition. The  $k-\omega$  model, along with the current method for modeling quasi-laminar boundary layers, was employed to supplement 104 cascade data sets from literature and in-house studies (i.e. Pratt & Whitney proprietary data) to build databases for attached- and separated-flow transition. Existing models for both transition mechanisms were assessed with the databases and deemed not to have sufficient accuracy for design purposes. Consequently, dimensional analysis was employed as a guide for the extraction of pertinent flow variables from flowfield predictions of the experiments, and new models were developed.

Two correlations were developed, one for the onset of attached-flow transition and the other for the length of a separation bubble prior to turbulent-reattachment. The current models are based on *local* flowfield parameters, and they appear to have greater efficacy than a number of extant correlations. In particular, the model for attached-flow transition appears to have a physical basis with respect to the fundamental mechanism of bypass transition in compressible flow. That is, it was found that the onset of transition occurs when the ratio of a boundary-layer diffusion time to a timescale associated with the local, energy-bearing turbulent fluctuations at the edge of the shear layer reaches a critical value. Further, it was found that the critical value of the ratio was nearly constant over a wide range of flowfield conditions consistent with turbomachinery airfoils. By contrast, no such underlying physical basis was apparent from considerations of the separated-flow model: it appeared to be more of a straight correlation of variables.

The models have been implemented as point-wise trips in a 3D RANS solver that forms part of a turbomachinery design-system. It

should be noted that both the attached- and separated-flow models are based solely on two-dimensional data and applications of them in three-dimensional flow fields may elucidate deficiencies. In addition, no modeling has been implemented to account for the effects of roughness on pre-transitional/separation boundary layers. Part II of this paper focuses on the validation of the current models for use in an airfoil design system

### ACKNOWLEDGEMENTS

The authors would like to thank Pratt & Whitney for granting permission to publish this work. In particular, they are grateful to Dr. Jayant Sabnis, Mr. Gary Stetson, and Mr. Joel Wagner for their support. Inspiration for this work is a result of the authors' participation in the Minnowbrook conferences that are sponsored by the U.S. Air Force Office of Scientific Research and NASA (See, e.g., NASA CP 1998-206958). Prof. T. V. Jones and Prof. Jim S.-J. Chen taught the authors the importance of starting any technical effort from basic principles, and additional insights were gleaned from discussions with A. A. Rangwalla, M. F. Blair, F. Ames, D. Zhang, L. Bertuccioli, and J. Duke.

### REFERENCES

- Abu-Ghannam, B. J. and Shaw, R., 1980, "Natural Transition of Boundary Layers - The Effects of Turbulence, Pressure Gradient, and Flow History," *IMEchE Journal of Mechanical Engineering Science*, Vol. 22, No. 5, pp. 213-228.
- Ames, F.E., 1994, "Experimental Study of Vane Heat Transfer and Aerodynamics in Elevated Levels of Turbulence," NASA Contract Report 4633.
- Ames, F.E., 1995, "Advanced k-epsilon Modeling of Heat Transfer," NASA Contract Report 4679.
- Ames, F. E. and Plesniak, M. W., 1995, "The Influence of Large Scale, High Intensity Turbulence on Vane Aerodynamic Losses, Wake Growth, and Exit Turbulence Parameters," ASME Paper No. 95-GT-290.
- Arts, T., de Rouvroit, L. M., and Rutherford, A. W., 1990, "Aero-Thermal Investigation of a Highly Loaded Transonic Linear Turbine Guide Vane Cascade," von Karman Institute for Fluids Dynamics Technical Note 174.
- Baines, W. D. and Peterson, E. G., 1951, "An Investigation of Flow Through Screens," *Transactions of the ASME*, Vol. 73, pp. 467-480.
- Blair, M. F., Werle, M.J., 1981, "Combined Influence of Freestream Turbulence and Favorable Pressure Gradients on Boundary Layer Transition and Heat Transfer," UTRC Report R81-914388-17.
- Boyle, R.J., Bunker, R.S. and Giel, P.W., 2003, "Predictions for the Effects of Turbulence on Turbine Blade Heat Transfer," ISABE Paper No. 2003-1178.
- Butler, T., Beaudoin, R., and Knight, P., 1988, "LPT Cascade Final Test Results, Inlet Turbulence Testing," P&W Report No. EII88-618-2166.
- Chen, K. K. and Thyson, N. A., 1971, "Extension of Emmons' Theory to Flows on Blunt Bodies," *AIAA Journal*, Vol. 9, No. 5, pp. 821-825.
- Clark, J. P., 1993, "A Study of Turbulent-Spot Propagation in Turbine-Representative Flows," D. Phil. Thesis, University of Oxford, Oxon., England.
- Clark, J. P., Jones, T. V., and LaGraff, J. E., 1994, "On the Propagation of Naturally-Occurring Turbulent Spots," *Journal of Engineering Mathematics*, Vol. 28, pp. 1-19.



- Davis, R. L., Carter, J. E., and Reshotko, E., 1985, "Analysis of Transitional Separation bubbles on Infinite Swept Wings," *AIAA Paper* 85-1685.
- Davis, R. L., Shang, T., Buteau, J., and Ni, R. H., 1996, "Prediction of 3-D Unsteady Flow in Multi-Stage Turbomachinery Using an Implicit Dual Time-Step Approach," *AIAA Paper* No. 96-2565.
- Dey, J. and Narasimha, R., 1990, "Integral Method for the Calculation of Incompressible Two-Dimensional Transitional Boundary Layers," *AIAA Journal of Aircraft*, Vol. 27, No. 10, pp. 859-865.
- Dhawan, S. and Narasimha, R., 1958, "Some Properties of Boundary Layer Flow During the Transition from Laminar to Turbulent Motion," *Journal of Fluid Mechanics*, Vol. 3, pp. 418-436.
- Drela, M., 1995, "MISES Implementation of Modified Abughanam/Shaw Transition Criterion," MIT Technical Report.
- Dunn, M. G., 2001, "Convective Heat Transfer and Aerodynamics in Axial Flow Turbines," *ASME Paper* No. 2001-GT-0506.
- Emmons, H. W., 1951, "The Laminar-Turbulent Transition in a Boundary Layer - Part 1," *Journal of the Aeronautical Sciences*, Vol. 18, pp. 490-498.
- Fraser, C. J., Higazy, M. G., and Milne, J. S., 1994, "End-Stage Boundary Layer Transition Models for Engineering Calculations," *Proceedings of the Institution of Mechanical Engineers*, Vol. 208, No. C3, pp. 47-58.
- Gier, J., Ardey, S., and Heisler, A., 2000, "Analysis of Complex Three-Dimensional Flow in a Three-Stage LP Turbine by Means of Transitional Navier-Stokes Simulation," *ASME Paper* No. 2000-GT-645.
- Gostelow, J.P. and Walker, G.J., 1991, "Similarity Behavior in Transitional Boundary Layers Over a Range of Adverse Pressure Gradients and Turbulence Levels," *ASME Journal of Turbomachinery*, Vol. 113, pp. 617-625.
- Gostelow, J.P., Blunden, A.R., and Walker, G.J., 1994, "Effects of Freestream Turbulence and Adverse Pressure Gradients on Boundary-Layer Transition," *ASME Journal of Turbomachinery*, Vol. 116, pp. 392-404.
- Halstead, D. E., Wisler, D. C., Okiishi, T. H., Walker, G. J., Hodson, H. P., and Shin, H. W., 1997, "Boundary Layer Development in Axial Compressors and Turbines: Part 3 of 4 - LP Turbines," *ASME Journal of Turbomachinery*, Vol. 119, pp. 225-237.
- Hatman, A. and Wang, T., 1999, "A Prediction Model for Separated Flow Transition," *ASME Journal of Turbomachinery*, Vol. 121, pp. 594-602.
- Herbert, T., 1988, "Secondary Instability of Boundary Layers," *Annual Review of Fluid Mechanics*, Vol. 20, pp. 487-526.
- Hinze, J. O., 1975, *Turbulence*, Second Edition, McGraw-Hill, New York, p. 272.
- Hofeldt, A. J., 1996, "An Investigation of Naturally-Occurring Turbulent Spots Using Thin-Film Gages," D. Phil. Thesis, University of Oxford, Oxon., England.
- Hofeldt, A. J., Clark, J. P., LaGraff, J. E., and Jones, T. V., 1998, "The Becalmed Region in Turbulent Spots," in *Minnowbrook II: 1997 Workshop of Boundary Layer Transition in Turbomachines*, NASA CP 1998-206958.
- Houtermans, R., Coton, T. and Arts, T., 2003, "Aerodynamic Performance of a Very High Lift LP Turbine Blade with Emphasis on Separation Prediction," *ASME Paper* No. 2003-GT-38802.
- Kim, J., Simon, T.W. and Kestoras, M., 1994, "Fluid Mechanics and Heat Transfer Measurements in Transitional Boundary Layers Conditionally Sampled on Intermittency," *ASME Journal of Turbomachinery*, Vol. 116, pp. 405-416.
- Lakshminarayana, B., 1991, "An Assessment of Computational Fluid Dynamic Techniques in the Analysis and Design of Turbomachinery - The 1990 Freeman Scholar Lecture," *ASME Journal of Fluids Engineering*, Vol. 113, pp. 315-352.
- Lax, P. D., and Wendroff, B., 1964, "Difference Schemes for Hyperbolic Equations with High Order Accuracy," *Communications on Pure and Applied Mechanics*, Vol. 17, pp. 381-398.
- Liepmann, H. W., 1943, "Investigations of Laminar Boundary Layer Stability and Transition on Curved Boundaries," *NACA Wartime Report* W-107 (also NACA ACR 3H30).
- Liepmann, H. W., 1945, "Investigation of Boundary Layer Transition on Concave Walls," *NACA Wartime Report* W-87 (also NACA ACR 4J28).
- Lou, W. and Hourmouziadis, J., 2000, "Separation Bubbles Under Steady and Periodic-Unsteady Main Flow Conditions," *ASME Paper* No. 2000-GT-0270.
- Mack, L. M., 1975, "Linear Stability Theory and the Problem of Supersonic Boundary Layer Transition," *AIAA Journal*, Vol. 13, No. 3, pp. 278-289.
- Massey, B. S., 1986, *Measures in Science and Engineering*, Ellis-Horwood, Ltd., Chichester, U.K., pp. 125-127.
- Mayle, R.E., 1991, "The Role of Laminar-Turbulent Transition in Gas Turbine Engines," *ASME Journal of Turbomachinery*, Vol. 113, pp. 509-537.
- Mayle, R. E. and Schulz, A., 1997, "The Path to Predicting Bypass Transition," *ASME Journal of Turbomachinery*, Vol. 119, pp. 405-411.
- Michelassi, V., Rodi, W., Giess, P.-A., 1998, "Experimental and Numerical Investigation of Boundary-Layer and Wake Development in a Transonic Turbine Cascade," *Aerospace Science and Technology*, No. 3, pp. 191-204.
- Morkovin, M. V., 1978, "Instability, Transition to Turbulence, and Predictability," *NATO AGARDograph* 236.
- Moss, R.W. and Oldfield, L.G., 1992, "Measurements of the Effect of Free-Stream Turbulence Length Scale on Heat Transfer," *ASME Paper* No. 92-GT-244.
- Narasimha, R., 1957, "On the Distribution of Intermittency in the Transition Region of a Boundary Layer," *Journal of the Aeronautical Sciences*, Vol. 24, pp. 711-712.
- Narasimha, R., 1985, "The Laminar-Turbulent Transition Zone in the Boundary Layer," *Progress in Aerospace Sciences*, Vol. 22, pp. 29-80.
- Narasimha, R., 1990, "Modeling the Transitional Boundary Layer," *NASA CR-187487*.
- Narasimha, R., 1991, "Recent Advances in the Dynamics of the Transition Zone", *ISABE Paper* No. 91-7006.
- Narasimha, R., 2003, "Review of Recent Research in Bangalore on the Transition Zone," to be published in *Minnowbrook IV: 2003 Workshop of Boundary Layer Transition in Turbomachines*, NASA Conference Proceedings.
- Ni, R. H., "Advanced Modeling Techniques for New Commercial Engines," 1999, XIV ISOABE Conference, Florence, Italy, 5-10 September.
- Owen, F.K., 1970, "Transition Experiments on a Flat Plate at Subsonic and Supersonic Speeds," *AIAA Journal*, Vol. 8, No. 3, pp. 518-523.
- Praisner, T. J. and Rangwalla, A., 2001, "RANS-Based Loss and Heat-Load Predictions with the  $k-\omega$  Turbulence Model," P&W Report No. TGM. 424.
- Praisner, T.J., Clark, J.P., Grover, E.A., Bertuccioli, L., and Zhang, D., 2003, "Challenges in Predicting Component Efficiencies in Turbines with Low Reynolds Number Blading," to be published in



*Minnowbrook IV: 2003 Workshop of Boundary Layer Transition in Turbomachines*, NASA Conference Proceedings.

Praisner, T. J., Grover, E. A., Rice, M. J., and Clark, J. P., 2004, "Predicting Transition in Turbomachinery, Part II – Model Validation and Benchmarking," ASME Paper No. GT-2004-54109.

Reshotko, E., 1976, "Boundary-Layer Stability and Transition," *Annual Review of Fluid Mechanics*, Vol. 8, pp. 311-349.

Roach, P. E. and Brierley, D. H., 2000, "Bypass Transition Modeling: A New Method Which Accounts for Freestream Turbulence Intensity and Length Scale," ASME Paper No. 2000-GT-278.

Roberts, S. K. and Yaras, M. I., 2003, "Measurements and Prediction of Freestream Turbulence and Pressure-Gradient Effects on Attached-Flow Boundary-Layer Transition," ASME Paper No. GT-2003-38261.

Roberts, W.B., 1980, "Calculation of Laminar Separation Bubbles and Their Effect on Airfoil Performance," *AIAA Journal*, Vol. 18, No. 1, pp. 25-31.

Roux, J., Lefebvre, M., and Liamis, N., 2002, "Unsteady and Calming Effects Investigation on a Very High Lift LP Turbine Blade – Part II: Numerical Analysis," ASME Paper No. GT-2002-30228.

Schlichting, H., 1979, *Boundary Layer Theory*, Seventh Edition, McGraw-Hill, New York, pp. 90-91, 470.

Schmidt, R.C. and Patankar, S.V., 1988, "Two-Equation Low-Reynolds-Number Turbulence Modeling of Transitional Boundary Layer Flows Characteristic of Gas Turbine Blades," NASA Contract Report 4145.

Schubauer, G.B. and Klebanoff, P.S., 1955, "Contributions on the Mechanics of Boundary Layer Transition," NASA TN-3489.

Sharma, O. P., Wells, R. A., Schlinker, R. H., and Bailey, D. A., 1982, "Boundary Layer Development on Airfoil Suction Surfaces," *ASME Journal of Engineering for Power*, Vol. 104, pp. 698-706.

Sharma, O. P., Renaud, E., Butler, T.L., Milsaps, K., Dring, R.P., and Joslyn, H.D., 1988, "Rotor-Stator Interaction in Multi-Stage Axial-Flow Turbines," *AIAA Paper No. 88-3013*.

Simon, F.F. and Ashpis, D.E., 1996, "Progress in Modeling of Laminar to Turbulent Transition on Turbine Vanes and Blades," NASA Technical Memorandum 107180.

Simoneau, R. J., and Simon, F. F., 1993, "Progress Towards Understanding and Predicting Heat Transfer in the Turbine Gas Path," *International Journal of Heat and Fluid Flow*, Vol. 14, pp. 106-128.

Solomon, W. J., Walker, G. J., and Gostelow, J. P., 1996, "Transition Length Prediction for Flows with Rapidly Changing Pressure Gradients," *ASME Journal of Turbomachinery*, Vol. 118, pp. 744-751.

Steelant, J. and Dick, E., 2001, "Modeling of Laminar-Turbulent Transition for High Free Stream Turbulence," *ASME Journal of Fluids Engineering*, Vol. 123, pp. 22-30.

Suder, K.L., O'Brien, J.E. and Reshotko, E., 1988, "Experimental Study of Bypass Transition in a Boundary Layer," NASA TM-100913.

Suzen, Y. B. and Huang, P. G., 2000, "Modeling of Flow Transition Using and Intermittency Transport Equation," *ASME Journal of Fluids Engineering*, Vol. 122, pp. 273-284.

Tani, I., 1969, "Boundary-Layer Transition," *Annual Review of Fluid Mechanics*, Vol. 1, pp. 169-196.

Thermann, H., Mueller, M., and Niehuis, R., 2001, "Numerical Simulation of Boundary Layer Transition in Turbomachinery Flows," ASME Paper No. 2001-GT-0475.

Van Driest, E. R. and Blumer, C. B., 1963, "Boundary Layer Transition: Free Stream Turbulence and Pressure Gradient Effects," *AIAA Journal*, Vol. 1, pp. 1303-1306.

Van Fossen, G.J., Simoneau, R.J., Ching, C.Y., 1994, "Influence of Turbulence Parameters, Reynolds Number, and Body Shape on Stagnation-Region Heat Transfer," NASA Technical Paper 3487.

Volino, R.J., 2002a, "Separated Flow Transition Under Simulated Low-Pressure Turbine Airfoil Conditions: Part 1 – Mean flow and Turbulence Statistics," ASME Paper No. 2002-GT-30236.

Volino, R.J., 2002b, "Separated Flow Transition Under Simulated Low-Pressure Turbine Airfoil Conditions: Part 2 – Turbulence Spectra," ASME Paper No. 2002-GT-30237.

Walker, G.J., Subroto, P.H., Platzer, M.F., 1988, "Transition Moeling Effects on Viscous/Inviscid Interaction Analysis of Low Reynolds Number Airfoil Flows Involving Laminar Separation Bubbles," ASME Paper No. 88-GT-32.

Walker, G.J., 1989, "Modeling of Transitional Flow in Laminar Separation Bubbles," *9<sup>th</sup> International Symposium on Air Breathing Engines*, pp. 539-548.

Walker, G. J. and Gostelow, J. P., 1990, "Effects of Adverse Pressure Gradients on the Nature and Length of Boundary-Layer Transition," *ASME Journal of Turbomachinery*, Vol. 112, pp. 196-205.

White, F. M., 1991, *Viscous Fluid Flow*, Second Edition, McGraw-Hill, New York, pp. 273-274.

Wilcox, D.C., 1988, "Reassessment of the scale-determining equation for advanced turbulence models," *AIAA Journal*, 26, 1299-1310.

Wilcox, D.C., 1998, *Turbulence Modeling for CFD*, Second Edition, DCW Industries, Inc., La Canada, California.

Yaras, M.I., 2002, "Measurements of the Effects of Freestream Turbulence on Separation-Bubble Transition," ASME Paper No. GT-2002-30232.